39th IAHR WORLD CONGRESS
GRANADA, SPAIN 2022
From Snow to Sea
19-24 June 2022

Proceedings of the 39th IAHR World Congress
19–24 June 2022, Granada, Spain
doi://10.3850/IAHR-39WC2521716X2022866

Numerical Modelling of Pump Intakes: Compliance with Standard Performance Criteria

Daniele Longo[(1)], Aggelos Dimakopoulos[(2)] and Ian Willoughby[(3)]

[(1)] HR Wallingford, Wallingford, UK,
d.longo@hrwallingford.com
[(2)] HR Wallingford, Wallingford, UK,
a.dimakopoulos@hrwallingford.com
[(3)] HR Wallingford, Wallingford, UK,
i.willoughby@hrwallingford.com

Abstract

In this work, we attempt to address some of the key questions regarding the applicability of CFD modelling for assessing the hydraulic performance of pumping installations and demonstration of compliance of the design against the criteria described in the ANSI/9.8-HI standards. We do this by re-visiting past experiments of pumping stations performed in HR Wallingford's laboratory and repeating these tests using CFD simulations with OpenFOAM. Existing workflows and analysis methods are used and new ones are proposed to assess the velocity profiles and swirl angles at the pump intakes and to characterise the relative strength of surface and subsurface vortices. Results show that the CFD model results can reproduce experimental data relating to the variation of velocity at the pump suctions within an average difference of ~2% and a maximum difference of ~4%, with the CFD model output showing a tendency to slightly overestimate the velocity profile variation. CFD output of swirl angles shows a good agreement with experimental trends as an overall indicator of facility performance, whilst variations were evident at individual pumps. The methodology proposed to assess CFD model results with respect to classification of surface and subsurface vortex strength presents a good correlation with laboratory observations. In overall terms, a good correlation between physical and CFD modelling results is achieved for assessing hydraulic performance of pump intakes against swirling flow, in the context of performance criteria described in the ANSI/HI-9.8 standards. The uncertainties of the methodology are also captured and further discussed.

Keywords: CFD modelling; Pump intakes; Swirling flows; Vortices; ANSI standards

1. INTRODUCTION

Pumping stations are hydraulic structures used in various types of critical infrastructure projects around the world, notably including cooling systems for power and industrial plants as well as drainage and wastewater management schemes. Amongst the various hydraulic design tasks performed for pumping station facilities, the mitigation of issues associated with swirling flows and the promotion of satisfactory entry flow conditions at the pump intakes is critical.

Previous studies of model and prototype pumping stations have demonstrated that facilities with poor approach conditions to the pumps and chambers prone to vortex formations, resulting in air entrainment and/or swirl at the pump suctions, can be the cause of severe operational difficulties, such as:

- increase in intake head losses;
- reduction in maximum intake rate due to vortex flow;
- deterioration of running efficiency of pump units due to fluctuations of velocities and pressure;
- stimulation of vibration and cavitation inception leading to wear and damage of pumping machinery.

Ensuring the absence of swirling flows at the pump suctions minimises the above adverse effects and promotes good working conditions, thus reducing maintenance and operational costs. Key performance indicators such as the variation of the velocity profile, swirl angles at the pump intakes, and absence of strong surface and subsurface vortices are typically used to assess issues associated with swirling flows. These are discussed in the ANSI/HI-9.8 standards, where it is also stated that these indicators are currently recommended to be assessed using physical models and not with CFD models. However, with the advance of CFD modelling tools, there is evidence that the engineering community is seeking a move towards increasing the use of CFD modelling. Notably, the work from Torbaty (2019) was a first step towards linking results from CFD modelling assessments to the Alden Research Laboratory (ARL) Vortex classification system (Knauss 1987), by developing correlation equations based on dimensional analysis and benchmarking of CFD model results with physical model data. Whilst this work presents an advance in the current state of the art, it does not address key questions regarding subsurface vortices, as well as compliance with other criteria described in ANSI-HI/9.8, such as swirl angles and pump throat velocity profiles

In this work, we made use of HR Wallingford's past physical modelling and CFD modelling data as a basis to re-analyse swirling flow patterns and assess compliance against the criteria described in the ANSI/HI-9.8 standards. The results of this study confirm the validity of the relation proposed by Torbaty (2019) and further extend it for application in subsurface vortex characterisation. In addition, analysis methods are proposed for assessing general compliance with throat velocity profiles and swirl angle criteria.

2. PHYSICAL AND NUMERICAL MODELLING OF PUMPING STATIONS

2.1 Physical Modelling

Physical models have been used to verify the hydraulic design of pumping station arrangements over many years and physical modelling currently remains the most reliable available technology to assess the performance of pumping station arrangements during the design process. Physical model output is typically used to demonstrate good pump entry flow conditions and compliance to the criteria referenced in the ANSI/HI-9.8 standards, such as the ARL vortex type classification (Knauss, 1987), swirl angle limits and velocity variation limits, which are presented in the list below. ARL type vortices are described in Table 1.

i. Surface vortex types ARL 1 and ARL 2 are considered acceptable. ARL 3 is considered to be the maximum allowable class of surface vortex. A vortex having a dye-core reaching the pump suction represents the initiation of coherent swirl from surface through to pump intake and thus represents a suitable demarcation between acceptable and unacceptable performance. Dye cores should be present for less than 50% of the time (for infrequent operating modes) and preferably less than 10% of the time (for more frequent/common operating modes). The occurrence of surface vortex type ARL 4, 5 or 6 is considered unacceptable.
ii. Subsurface vortex type ARL 1 is considered acceptable. A subsurface vortex type ARL 2 is considered to represent the limit for acceptable performance. Repeated/frequent occurrence of stable ARL 2 (subsurface) vortices is considered unacceptable. ARL 3 vortices are unacceptable.
iii. The allowable angle of swirl in pump suctions may depend upon the particular characteristics of the prototype pump being used, and can be defined with reference to relevant pump manufacturer requirements. However, it is generally accepted that a safe limit for the swirl angle is 5°. Maximum swirl angles of up to 7° may be considered acceptable for infrequent pump operating conditions.
iv. Spatial/temporal variation of the velocity in the pump suction throat approaching the impeller location is considered acceptable within ±10% of the mean velocity.

Table 1. Alden Research Laboratory (ARL) vortex type classification

SURFACE VORTICES	**ARL 1**	Surface vortices taking the form of a surface rotation
	ARL 2	Small depression in the water surface with a non-coherent core
	ARL 3	Surface dimple with a relatively coherent core extending from surface to pump suction
	ARL 4	Surface vortex capable of pulling floating debris from the surface to pump inlet
	ARL 5 - ARL 6	Air-entraining (air bubble or full air core) surface vortices
SUBSURFACE VORTICES	**ARL 1**	Subsurface flow rotation
	ARL 2	Subsurface vortex having a central core that approaches a stable condition (coherent dye-core reaching the pump suction)
	ARL3	Subsurface vortex capable of drawing air from solution

2.2 Numerical Modelling

Advances in numerical methods and computational power over recent years have resulted in the development of computational fluid dynamic (CFD) tools that can reduce the time and costs involved in the design optimisation and validation of complex hydraulic structures. CFD models are numerical models that resolve the 3D Navier Stokes equations and therefore, when used appropriately, can be considered as a "virtual laboratory". Despite their inherent limitations, relating to simplifying assumptions and computational cost, they present several advantages over physical models, such as access to a wide range of predicted flow data (e.g. velocities, pressures, turbulence and mixing variables), non-intrusive sampling of flow data and production of 3D visual outputs that may aid interpretation of complex flow structures. In addition, unlike a physical model (which will typically be dismantled after the conclusion of the study), the CFD model can remain available during the entire design and operational lifetime of the structure, and any modifications pertinent to future design improvements can be assessed at a relatively low time and cost burden.

CFD simulations for pumphouse arrangements have to date been valuable when assessing general flow paths within a pumping station and for optimising the general size and shape of an installation. An example is presented in Figure 1, where, based upon the results obtained from the CFD modelling study, it was concluded it may be required to introduce arrays of baffles in order to promote satisfactory operating conditions at the pumps, in addition to anti-vortex devices at the pump suctions.

It is nevertheless noted that, at the time of developing the present study, the use of CFD modelling is not recommended to demonstrate compliance with criteria described in the ANSI/HI-9.8 standards relating to swirling flows and vortex action at pump intakes. So in the example of Figure 1, the final configuration for the required baffle arrangements and local anti-vortex devices was subsequently confirmed by an extensive and time-consuming physical modelling study. In this study, we aim to further improve the reliability of CFD modelling as a stand-alone tool by demonstrating that it can be used to provide valuable insights with respect to hydraulic performance and compliance relative to the criteria described in the ANSI/HI-9.8 standards.

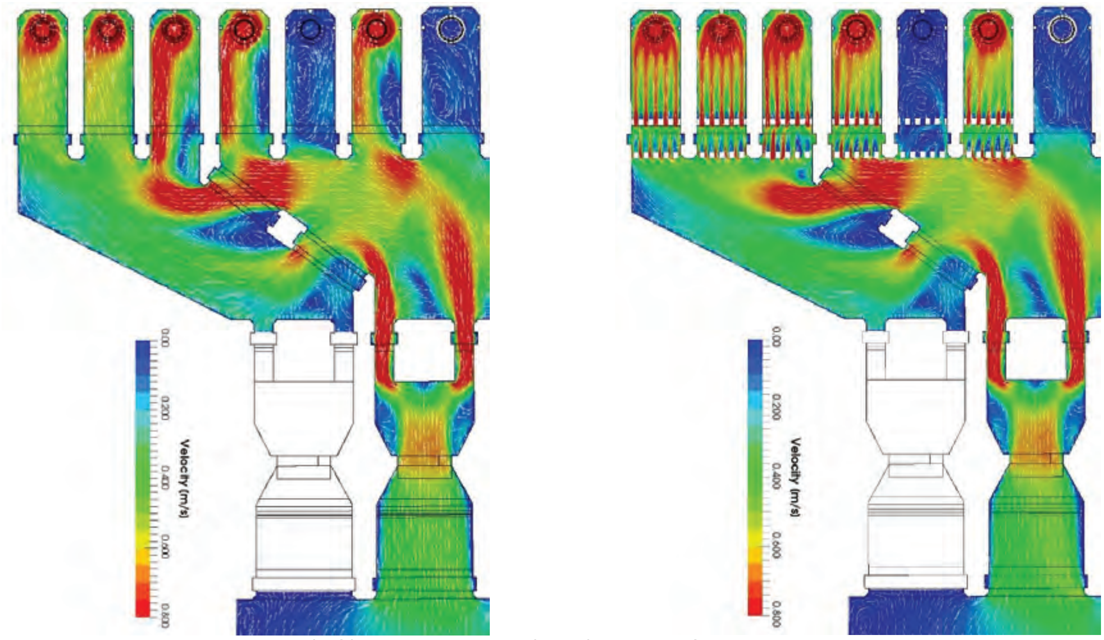

Figure 1. Example original (left) and optimised (right) layout of pump chambers.

3. MODEL SET-UP & ANALYSIS METHODS

3.1 Model Setup

In this work, we used the OpenFOAM® CFD platform (www.openfoam.org), to model three previously physically modelled pumping stations and perform comparisons with past experimental data. The 3D geometry for the CFD models corresponded to the physical model structure (at model scale). The geometry was generated on the basis of available information from the associated physical model studies, which are anonymised for the purposes of this publication. The numerical model geometry represented the physical model structure as closely as possible, although several simplifications on the geometry were made, by omitting features or flow areas of little importance. The free-surface was modelled as a fixed-lid approximation. This is an approach most commonly used by the industry for CFD modelling of pumping stations as this is more computationally efficient than modelling approaches with free-surface tracking, as it provides a very good approximation of the flow near the free-surface when the disturbances in the water surface are small (compared with the water depth). Therefore, the numerical domain was built to include only the water phase with the top boundary of the domain representing the free surface location.

The computational model mesh was generated using snappyHexMesh, the built-in OpenFOAM mesher. Initial mesh parameters were defined according to past experience and relevant mesh sensitivity tests performed within the framework of this study, that are not shown here. The simulations were set-up for single phase flow and for all cases the fluid was considered as freshwater at 10° C; with the kinematic viscosity set to 1.29 x 10^{-6} m^2/s. Turbulence properties were accounted for by using the RAS (Reynolds-averaged stress) k-omega-SST model (Menter 1994) according to previous experience and sensitivity analyses performed in equivalent pumping stations. The SST model effectively blends the formulation of the k-omega model in the near-wall region with the free-stream independence of the k-epsilon model in the far field, making it a relatively well-balanced turbulence model for most applications. See Pope (2000) for a more detailed evaluation of RAS models.

A combination of wall, inlet and outlet boundary conditions were used to represent the different flow boundaries (inflow/outflow planes, walls, free surface). All the surfaces were treated as solid walls and no-slip condition was enforced coupled with turbulent wall functions for calculating near-wall turbulent characteristics, including effects of roughness. In this case, we assumed smoothed walls, which is a suitable approximation, given the low roughness materials (smooth painted plywood or Perspex) that are preferred in physical models.

A total of 3 pumping stations typically comprising 3-4 pumps each were simulated following a test programme of 16 simulations in total (5-6 simulations per pumping station). This created a database of >50 pump intake assessments which were analysed according to the methods presented in the next section.

3.2 Analysis Method

Swirl angles calculation

As part of a physical model study for a pumping station, the angle of swirl in the flow entering the pump suctions is measured on the basis of methods similar to those described in the ANSI/HI-9.8 standard. In particular, the measurement of the intensity of the swirl angle, α, representing the intensity of flow rotation, is determined using a rotary swirl meter. The rotor has vanes with zero pitch (see Figure 2, right) and it is installed in the suction arrangement. The swirl angle is proportional to the number of rotor revolutions per second through the following relation:

$$\alpha = \tan^{-1}\frac{\pi 2Rn}{V_z} \quad [1]$$

where:

$2R$ is the pump suction diameter or rotor diameter
V_z is the axial flow velocity
n is the number of revolutions per second

The allowable angle of swirl is generally accepted as having a limit of 5°. Maximum swirl angles of up to 7° may be considered acceptable for infrequent pump operating conditions. In this study an approach for extracting the swirl angle in the CFD model is proposed. This is based on use of existing formulations (Mitra et al 2015) to quantify the rotational momentum and to correlate this with the rotor rotation. This essentially allows the physical representation of the rotor to be omitted from the CFD modelling procedure.

According to Mitra et al (2015), the swirling angle in CFD models can be calculated as follows:

$$\alpha = \tan^{-1}\left(\frac{\omega R}{V_z}\right) \quad [2]$$

and

$$\omega = \frac{\int_A (\boldsymbol{r} \times \boldsymbol{v})(\rho \boldsymbol{v} \cdot \hat{n} dA)}{\int_A r^2 \,(\rho \boldsymbol{v} \cdot \hat{n} dA)} \quad [3]$$

where:

ω is the bulk angular velocity
R is the pump inlet radius or rotor radius
r is a position vector measured from the axis of the rotor
v is the velocity vector in cartesian coordinate frame
$\hat{n}$ is the unit vector aligned with the main flow direction
A is the control area or volume

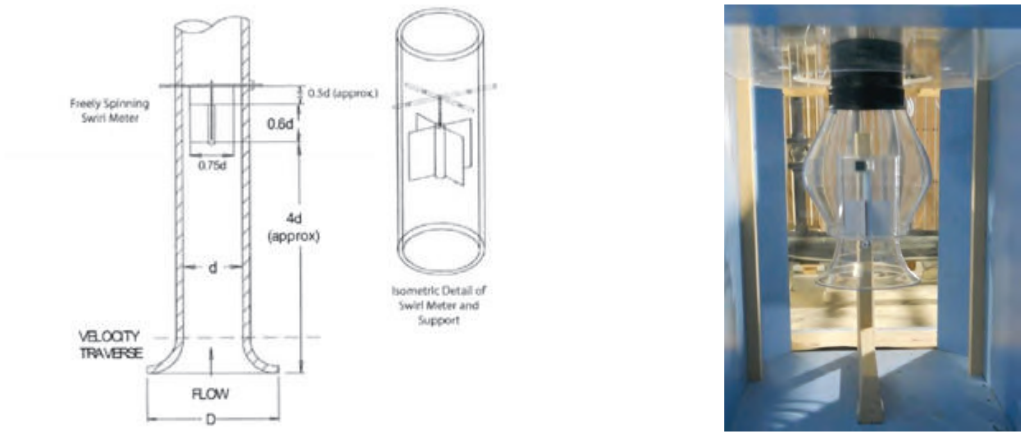

Figure 2. Swirl meter installation scheme as per ANSI/HI-9.8 standard (left) and example swirl meter installation in a physical model (right).

In this study, it was considered that the swirl angle calculated using equation [3] at the volume occupied by the swirl meter rotor was nominally equivalent to that derived from physical model measurements. A new set of libraries and solvers was developed in OpenFOAM so as to include the swirl angles as a direct output of the CFD model. The calculation method (equation [3]) from Mitra et al (2015) was embedded in the CFD model solution over a control volume that has a cylindrical shape and covers the same extent as the rotor.

Flow velocity profiles in pump intakes

In a physical model study, velocity profiles at the pump suction throat are measured using Pitot tubes connected across differential pressure transducers. These measurements are performed along specific axes (generally 2, 3 or 4 axes) so as to enable assessment of mean and fluctuating velocities and therefore to confirm satisfactory spatial velocity distribution and temporal velocity variation at the pump suctions. In assessing the hydraulic performance of an intake, the variation in the pump throat velocity within ±10% of the mean velocity is acceptable according to the ANSI/HI-9.8 standards.

In a CFD model, the spatial velocity distribution and variation at the pump suctions can be assessed by means of non-intrusive sampling. It is nevertheless noted that performing reliable near wall sampling in the CFD model may be dependent on the local mesh size. Additionally, it can also be the case that Pitot tubes positioned close to the sidewalls have some (modest) modifying influence ("intrusion" effects) to the flow in a physical model due to their very close location adjacent to the sidewall of the pump intake. On this basis, axial velocity comparisons close to the sidewall were omitted in evaluating the criterion, whilst uncertainty of the near-wall velocities is further commented upon below.

Surface/subsurface vortices calculation

In a physical model of a pumping station, the potential onset of surface and/or subsurface vortices at pump intakes is typically determined based on visual observations, supported by using injected dye tracers. Still photographs and video recording techniques are also used to supplement visual observations. The ARL vortex classification (see Table 1) and associated compliance with the ANSI criteria constitutes an output of the physical modelling study, on the basis of the observations mentioned above.

In a CFD model of a pumping station, post-processing vortex identification and visualisation techniques can be used to identify the potential occurrence of surface and subsurface vortices at pump intakes. In this study, vortex analysis made use of the well-known Q-criterion (Hunt et al 1988) as a vortex identification technique that essentially compares the local vorticity against the strain rate. The areas with $Q > 0$ belong in coherent vortices. Although it is evident that the larger the value of Q, the stronger the vortex, the relative strength of the vortex (in the context of the ARL vortex classification shown in Table 1) cannot be solely assessed by Q. Images showing predicted/potential vortex core lines (Sujundi and Haimes 1995; Levy et al 1990) can also be used in conjunction/combination with the Q-criterion parameter to obtain more substantive evidence of the potential for occurrence of coherent surface and subsurface vortices at pump intakes. The vortex core line represents its possibly rotational axis around which the flow spirals. An example visualisation is shown in Figure 3 where both the output of Q-criterion and vortex cores filter are shown near the pump intake.

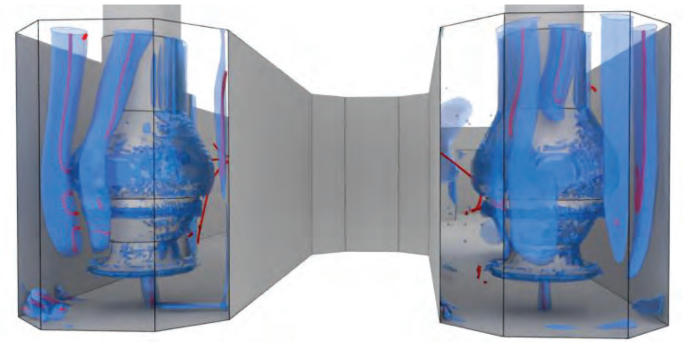

Figure 3. Example of Q-criterion field (blue) and vortex core lines (red) to identify any coherent vortical structure at the pump chambers

Vortex identification techniques can be used in the context of hydraulic structures and pumping stations along with a characterisation methodology to assess the significance of the vortex (Zhan et al 2019; Torbaty 2019). In particular, a Vortex Risk Index (VRI) is proposed by Torbaty (2019) for single phase models of pump intakes, which uses dimensional analysis to classify vortices according to the risk they pose in a particular intake. The formula used is the following:

$$T_o = K_s \frac{\nu^{0.2}\sqrt{\omega_m}}{gS^2}\left(\frac{Q}{D}\right)^{1.3} \qquad [4]$$

where:

- T_o is the VRI value
- ω_m is the maximum vorticity at the vortex eye
- S is the pump submergence
- Q is the intake discharge
- D is the intake bellmouth diameter
- K_s is a scaling coefficient equal to 1000 (Torbaty 2019)

Most of the variables above can be readily retrieved by the pumping station layout and operational conditions, except the variable ω_m, which must be calculated from post-processing analysis of the CFD results. In particular, a vortex identification criterion must be used to define the vortex eye at the free-surface and the maximum vorticity. According to Torbaty (2019) the values of T_o are used to classify the pump intake according to the following risk zones:

- the low-risk zone for T_o < 1.27 (correlated with ARL Type 1/2 surface vortex)
- the high-risk zone for T_o > 3.45 (correlated with > ARL Type 4 surface vortex)
- the middle zone 1.27 < T_o < 3.45 where vortices may fluctuate between ARL Type 2-4 surface vortex

It is noted that the method from Torbaty (2019) was not originally developed for subsurface vortices. In this study, a modified form of this method has been introduced for characterising subsurface vortices and its applicability is assessed against experimental predictions. The form of the equation has been kept similar to that of equation [4], with the following changes:

- Instead of the submergence *S*, we will use the distance *L* from bellmouth to the wall boundary, along the vortex path.
- ω_m is calculated at the vortex eye at the wall boundary
- K_s should be adapted, so that T_o is aligned with the ARL classification for subsurface vortices

Equation [4] is therefore modified for application to subsurface vortices as follows:

$$T_{o,sub} = K_{s,sub} \frac{\nu^{0.2}\sqrt{\omega_m}}{gL^2}\left(\frac{Q}{D}\right)^{1.3} \qquad [5]$$

After performing preliminary analysis, it was proposed that $K_{s,sub} = 20$, such that the following criteria apply.

- $T_{o,sub}$ < 1 can be assessed as a "low risk zone" (correlated with ARL Type 1 (or less) subsurface vortex)
- $T_{o,sub}$ > 2 can be assessed as a "high risk zone" (correlated with ARL Type 2 (or greater) subsurface vortex)
- 1 ≤ $T_{o,sub}$ ≤ 2 can be assessed as an "intermediate risk zone" (where subsurface vortices may fluctuate between ARL Type 1 and ARL Type 2).

For the ARL classification output, we combine the use of the Q-criterion and the VRI index in order to identify and characterise surface vortices according to risk of occurrence, and compare predictions with physical model observations to confirm the analysis output.

4. RESULTS AND COMPLIANCE WITH ANSI/HI-9.8 STANDARDS PERFORMANCE CRITERIA

4.1 Compliance with Velocity Criteria

To sample the spatial distribution of velocity at the pump throat, numerical probes were placed in the model domain at the same positions along the axis where the pitot tubes were placed in the physical model. The mean (corresponding to time-averaged) velocity values at each location were then compared with the physical model results. An example of the velocity profile comparison and relative percentage error is presented in Figure 4. The use of CFD model for assessing the (spatial) variation of the time averaged velocity profile is considered appropriate and viable. Benchmarking with physical models showed a mean level of deviation at ~2% and a maximum deviation of ~4% (normalised to the mean flow velocity). The CFD model profiles tended to show a greater variation than the physical model profile, which indicates that CFD model results generally erred toward the conservative side. It is therefore reasonable to consider that if a pump intake layout meets the <10% variation criterion in the CFD model, it is likely that the criterion would also be satisfied in the physical model.

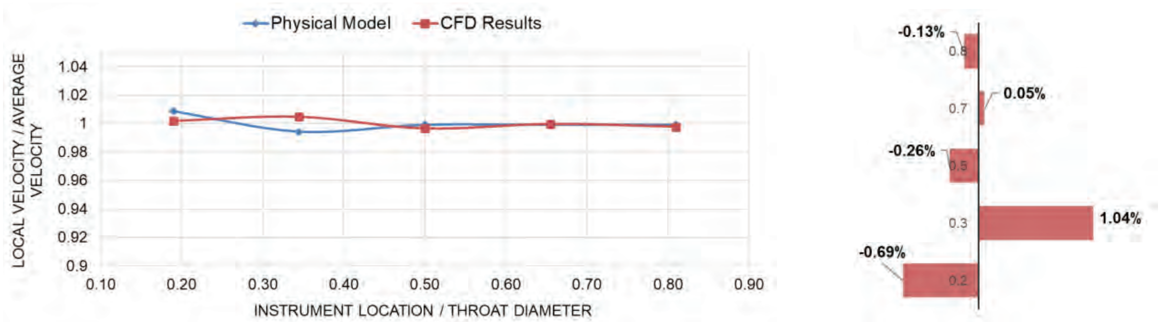

Figure 4. Example of pump suction velocity variations –Profile comparison (left) and relative percentage error (right)

During the analysis, it was noted that the comparison of near-wall velocities between the CFD and the physical model generally showed a much larger discrepancy, e.g. towards ~10% compared to the mean velocity. In relation to near-wall velocities it was considered that the CFD model was tending to pick-up a slightly extended boundary layer compared to the physical model. This was potentially considered to be due to the relatively few mesh cells used at near-wall locations, or potentially due to the mild flow interference of a Pitot tube near the wall having influence on the physical model data. Given the apparent uncertainties, we chose not to include near-wall locations when evaluating the velocity criterion. In order to resolve the uncertainties, the CFD model should probably include the Pitot tube geometry, along with a much higher near-wall refinement of the mesh, which was outside of the scope of this study.

4.2 Compliance with Swirl Angle Criteria

Comparison between CFD and physical model results showed that the variation trends for swirl angles were well captured by the CFD model (e.g. variation with water level, variation due to applied anti-vortex measures), but variations and discrepancies between individual pumps were noted. The general agreement between CFD model and physical model was improved when considering an “overall performance assessment” for the pumping station, by considering the average of predicted swirl angles across pumps, but some discrepancies still exist.

It is noted here that measurements and observations in a physical model are typically focussed on characterising “highest” measured swirl angles at each pump position during relevant tests – so as to conclude a conservative assessment. Intrinsic turbulence and fluctuations in the flow patterns approaching and within pump chambers result in time varying fluctuations of the swirl angle. Typically, several sets of measurements will be made in the physical model where swirl angles may be averaged over periods of a few minutes. Short-term bursts of swirl (over short periods of perhaps 10-30 seconds in model time) are also assessed. Worst-case (“highest”) values are reported to provide for a suitably conservative assessment. In this respect, it should be generally expected that CFD modelling based on steady-state run simulations may not capture the precise values documented in physical modelling outputs and an averaged correlation should be sought in relation to validation of the CFD predictions.

In addition, the steady state CFD solution of what can be intrinsically unsteady flows, such as those that exist in pumping stations, may result in some "variation" of the solution during the convergence process. These variations typically appear in areas of high "unsteadiness", which, in the present case, coincide with the areas of potentially high swirling flows. This adds an additional layer of uncertainty, as, in theory, all of the varying solutions may be considered as a valid representation of the flow field. To help mitigate the uncertainty we recorded the high, median and low swirl angle, as the numerical solution evolves beyond convergence stage. An example of the swirl angle analysis for each scenario is shown in in Figure 5.

Table 2 summarises the overall discrepancies observed comparing CFD and physical model predictions, using the averaged values of swirl angles across all pumps. Modification factors (MF) are calculated, based on the CFD and physical model results, and used to "correct" the min, max and mid-range CFD results toward an improved correlation with physical model values. The RMS variations between the physical and numerical model output are also presented, normalised to mean physical model swirl angle value. It is shown that, typically, the max, mid-range and min CFD results differ by 12%, 6% and 34% with respect to the physical model results. The normalised RMS variation ranges from 26% to 40%. The CFD min value shows a relatively larger discrepancy when compared with the physical model results, and hence the min value is not considered further in the analysis – noting that as indicated above, the physical model studies will typically document "significant" (e.g. from average to highest) values and hence correlation with minimum values should not be expected.

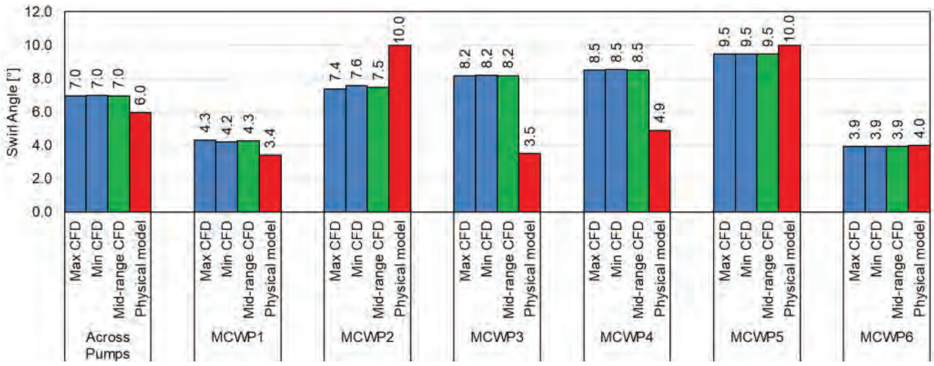

Figure 5. Example of absolute values of the max, min and mid-range swirl angle measured at the pumps in the CFD simulations.

Table 2. Swirl Angles - Analysis of errors. Values in degrees

Case	Max CFD	Min CFD	Mid-range CFD	Physical model	Error Mid	Error Max	Error Min
Case 01 – Test 1	7.3	4.4	5.9	4.5	31%	62%	-2%
Case 01 – Test 2	3.4	1.5	2.4	2.9	-17%	17%	-48%
Case 01 – Test 3	4.2	3	3.6	4.7	-23%	-11%	-36%
Case 01 – Test 4	10.5	3.3	6.9	6.9	0%	52%	-52%
Case 01 – Test 5	3.6	1.3	2.5	2.5	0%	44%	-48%
Case 02 – Test 1	6.1	3.2	4.7	3.7	27%	65%	-14%
Case 02 – Test 2	5.1	3.4	4.2	7.2	-42%	-29%	-53%
Case 02 – Test 3	2.6	1.4	2	2.9	-31%	-10%	-52%
Case 02 – Test 4	3.8	0.2	2	2.6	-23%	46%	-92%
Case 02 – Test 5	6.8	3.2	5	5.3	-6%	28%	-40%
Case 03 – Test 1	5.9	5.2	5.5	7.1	-23%	-17%	-27%
Case 03 – Test 2	7	6.9	7	6	17%	17%	15%
Case 03 – Test 3	2.8	1.7	2.2	1.3	69%	115%	31%
Case 03 – Test 4	1.8	0.8	1.3	1.2	8%	50%	-33%
Case 03 – Test 5	6.4	5.9	6.2	6.2	0%	3%	-5%
Case 03 – Test 6	2.3	1.2	1.7	1.9	-11%	21%	-37%
Mean	4.76	3.12	3.94	4.18			
Modification factor MF (%)	88%	134%	106%				
RMS	1.67	1.65	1.09				
RMS (%)	40%	39%	26%				

4.3 Compliance with ARL Vortex Classification

The ARL vortex strength classification was evaluated for the entirety of the pumping station, by considering the most adverse conditions, in terms of vortex formation, in any of the pumps, for each scenario. The results of T_o and $T_{o,sub}$ (equations [4] and [5]) and VRI classifications are compared with the assessment of the physical model in Table 3. In general a very good agreement was observed, with the CFD-based assessment correlating relatively well with the physical model observations. There are two cases (Case 01-Test 2 and Case 01-Test 5) where the CFD output results in a more conservative assessment than the physical model. It is nevertheless noted that for this case the physical model indicated the presence of relatively strong vortices behind the pump intake within the pump chambers, but it was not assessed that these vortices were air entraining.

Table 3. Summary output of ARL assessment

<table>
<tr><th></th><th colspan="3">ARL Vortex classification (surface)</th><th colspan="3">ARL Vortex classification (subsurface)</th></tr>
<tr><th></th><th>T_o</th><th>VRI classification</th><th>Physical model</th><th>$T_{o,sub}$</th><th>VRI classification</th><th>Physical model</th></tr>
<tr><td>Case 01 – Test 1</td><td>0.3</td><td>Type 1/Type 2</td><td>Type 1/ Type 2</td><td rowspan="5">0.95</td><td rowspan="5">Type 1</td><td rowspan="5">Type 1/ Type 2</td></tr>
<tr><td>Case 01 – Test 2</td><td>8</td><td>Type 4 and higher</td><td>Type 1/ Type 2</td></tr>
<tr><td>Case 01 – Test 3</td><td>0.3</td><td>Type 1/Type 2</td><td>Type 1/ Type 2</td></tr>
<tr><td>Case 01 – Test 4</td><td>0.3</td><td>Type 1/Type 2</td><td>Type 1/ Type 2</td></tr>
<tr><td>Case 01 – Test 5</td><td>3</td><td>Type 2/Type 4 (fluctuating)</td><td>Type 1/ Type 2</td></tr>
<tr><td>Case 02 – Test 1</td><td>0.9</td><td>Type 1/Type 2</td><td>Type 1/ Type 2</td><td rowspan="5">7.5 (before AVD measures)
~0 (after AVD measures)</td><td rowspan="5">Type 3 (before AVD measures)
Type 0/1 (after AVD measures)</td><td rowspan="5">Type 3 (before AVD measures)
Type 0/1 (after AVD measures)</td></tr>
<tr><td>Case 02 – Test 2</td><td>1.1</td><td>Type 1/Type 2</td><td>Type 1/ Type 2</td></tr>
<tr><td>Case 02 – Test 3</td><td>3.1</td><td>Type 2/Type 4 (fluctuating)</td><td>Type 2/ Type 3</td></tr>
<tr><td>Case 02 – Test 4</td><td>3.1</td><td>Type 2/Type 4 (fluctuating)</td><td>Type 2</td></tr>
<tr><td>Case 02 – Test 5</td><td>1.2</td><td>Type 1/Type 2</td><td>Type 1/ Type 2</td></tr>
<tr><td>Case 03 – Test 1 to Test 6</td><td>~0-0.5</td><td>Type 1</td><td>Type 1/ Type 2</td><td>0.64</td><td>Type 1</td><td>Type 1</td></tr>
</table>

5. CONCLUSIONS AND RECOMMENDATIONS

A methodology is proposed to assess the output of CFD simulations for the purpose of assessing compliance with performance criteria described in the ANSI/HI-9.8 Standards. The methodology was applied to CFD simulation output for 3 pumping station layouts and for 16 operational scenarios (in total) and results were compared with available corresponding physical modelling observations. In general, good correlation was found between CFD and physical model data, thus providing some confidence that the methodology can be used to demonstrate general compliance with ANSI standards, subject to the following recommendations.

- Regarding the flow velocity profile in the pump throat:
  - The CFD model results were within 2% (on average) of the physical model profile, with the CFD model predicting a slightly more conservative assessment. It is therefore concluded that the CFD model output can be used for assessing general compliance with the criterion relating to a maximum ±10% spatial variation in the velocity.
  - Near-wall velocity readings (subject to boundary layer flow) should not be taken into account in the assessment, as further work is needed to justify the differences between CFD model and physical observation data (e.g. more refined models, inclusion of potential near-wall intrusive effects).
  - The numerical solution approach for the CFD simulations is based on steady-state flow assumptions, hence it is not appropriate to assess temporal deviation criteria, with respect to the velocity profile. This could be better achieved with an unsteady RANS or LES approach, which are probably more time consuming than the approach proposed herein. Additional work may be pursued to investigate compliance to temporal criteria. It is also noted, however, that available physical modelling data tends to show spatial variations in velocity generally have greater magnitude than temporal variations.
- The assessment for the swirl angle criteria is subject to a degree of uncertainty, on a case by case basis, even though the overall averaged results show a good agreement with the laboratory data. For this reason, in Table 2, we calculated the modification factor (MF) and the root mean square (RMS) error relative to the physical modelling data using the entire test database. A simplified assessment process can be applied to evaluate general compliance with swirl angle criterion using the CFD-predicted performance.

  - If any of the pump intakes modelled presents max swirl angles >5° (or >7° for infrequent operating modes), the design would be considered to likely fail to meet the ANSI/HI-9.8 standard criteria, and mitigation measures would be considered and proposed.
  - If all the pump intakes modelled present max swirl angles <5° (or <7° for infrequent operating modes), but the overall averaged mid-range swirl angle is >3.6° (or >5° for infrequent operating modes), the design would be considered to likely fail to meet the ANSI/HI-9.8 standard criteria, and mitigation measures would be considered and proposed.
  - If all pump intakes present max swirl angles <5° (or <7° for infrequent operating modes), and the overall averaged mid-range swirl angle is <3.6° (or <5° for infrequent operating modes), the design would be considered likely to meet the ANSI/HI-9.8 standards, and modifications would not be considered necessary.

  It is noted that the reduced limiting value of >3.6° (or >5° for infrequent operation) is proposed to take into account the modification factor and root means square error (MF + 1xRMS ≈ 1.4). This approach was found to provide good agreement with the physical modelling assessment for 80% of the cases considered, and for cases of disagreement, the CFD model provided a more conservative assessment.
- For evaluation of surface vortices, the methodology proposed by Torbaty et al (2019) was confirmed, so the use Equation [4] is recommended to calculate the Vortex Risk Index (VRI) or T_o, where:
  - for T_o < 1.27 can be correlated with ARL Type 1/2 vortices;
  - for T_o > 3.45 can be correlated with ARL Type 4 surface vortex or higher;
  - for 1.27 < T_o < 3.45 can be correlated with fluctuating ARL Type 2-4 surface vortex;
  - and therefore, for T_o>1.27 (fluctuating Type 2/3 or higher), improvement measures should be considered to reduce risks of occurrence of unacceptably strong surface vortex formations.
- Similarly, for subsurface vortices following the adapted VRI methodology proposed herein, we can use Equation [5] to calculate the Vortex Risk Index for subsurface vortices or $T_{o,sub}$, where:
  - for $T_{o,sub}$ < 1 can be correlated with ARL Type 1 (or less) subsurface vortex;
  - for $T_{o,sub}$ > 2 can be correlated with ARL Type 2 (or greater) subsurface vortex;
  - for 1 < $T_{o,sub}$ <2 can be correlated with fluctuating ARL Type 1 to ARL Type 2 subsurface vortices;
  - and therefore, for $T_{o,sub}$>1 (fluctuating Type 1/2 or higher), improvement measures should be considered to reduce risks of occurrence of unacceptably strong surface vortex formations.

6. ACKNOWLEDGEMENTS

This work was funded by HR Wallingford's internal research programme – project SWIrling Flows and Turbulence in Pumps (SWIFT Pumps), project No DKY0570. The authors acknowledge the help from Mr Andi Karanxha in retrieving past physical modelling data and the feedback by Mr Antonino Scala when applying the methods in recent design studies for pumping stations.

7. REFERENCES

ANSI/HI 9.8 (2018). *American National Standard for Rotordynamics in Pumps.* Hydraulic Institute, NJ

Hunt, J. C. R., Wray A. A. , and Moin P. (1988). *Eddies, stream, and convergence zones in turbulent flows*. Report CTR-S88." Center for Turbulence Research.

Knauss J. (1987). Swirling Flow Problems at Intakes, CRC Press

Levy Y, Degani D, Seginer A (1990). Graphical visualization of vortical flows by means of helicity. *AIAA journal*, 28 (8),1347–1352

Menter F. R. (1994), Two-Equation Eddy-Viscosity Turbulence Models for Engineering Applications, *AIAA Journal*, 32 (8), 1598-1605.

Mitra, P., Gudibande, N., Iyer, K. and Eldho, T.I. (2015). Algorithm for estimating swirl angles in multi-intake hydraulic sumps.

Torbaty M.A. (2019) Development of a Vortex Risk Index for Use with Single-phase Computational Fluid Dynamics in the Simulation of Intake Structures, *PhD thesis*, UNSW, Sydney.

Pope S.B. (2000). *Turbulent flows*. Cambridge university press.

Sujudi D, Haimes R (1995). Identification of swirling flow in 3-D vector fields. *In 12th Computational Fluid Dynamics Conference,* 1715, 1995

Zhan, J.M., Li, Y.T., Wai, W.H.O. and Hu, W.Q., (2019). Comparison between the Q criterion and Rortex in the application of an in-stream structure. *Physics of Fluids*, 31(12), 121701

